Proteasome Inhibition Reduces NBR1 Protein Levels in mATG8-Deficient Cells Independently of Lysosomal Degradation and RAB27A

Cerda-Troncoso C. (1)⚓, Arias-Muñoz E. (1), Vargas G. (1), Gaete-Ramírez M. (1,2), Cereceda K. (1), Cavieres VA. (1)¶ and Burgos PV. (1,2)¶

1. Centro de Biología Celular y Biomedicina CEBICEM, Facultad de Ciencias, Universidad San Sebastián, Avenida del Valle Norte 725, Santiago 8580704, Chile.
2. Centro Científico y Tecnológico de Excelencia Ciencia & Vida, Facultad de Medicina y Ciencia, Universidad San Sebastián, Avenida del Valle Norte 725, Santiago 8580704, Chile.

⚓ **Current address.**
Laboratory for extracellular vesicle research, Department of Human Genetics, KU Leuven. O&N6, Herestraat 49 box 610, 3000 Leuven, Belgium.

¶ **Corresponding authors.**
Cavieres VA, email: viviana.cavieres@uss.cl
Burgos PV, email: patricia.burgos@uss.cl

Graphical abstract

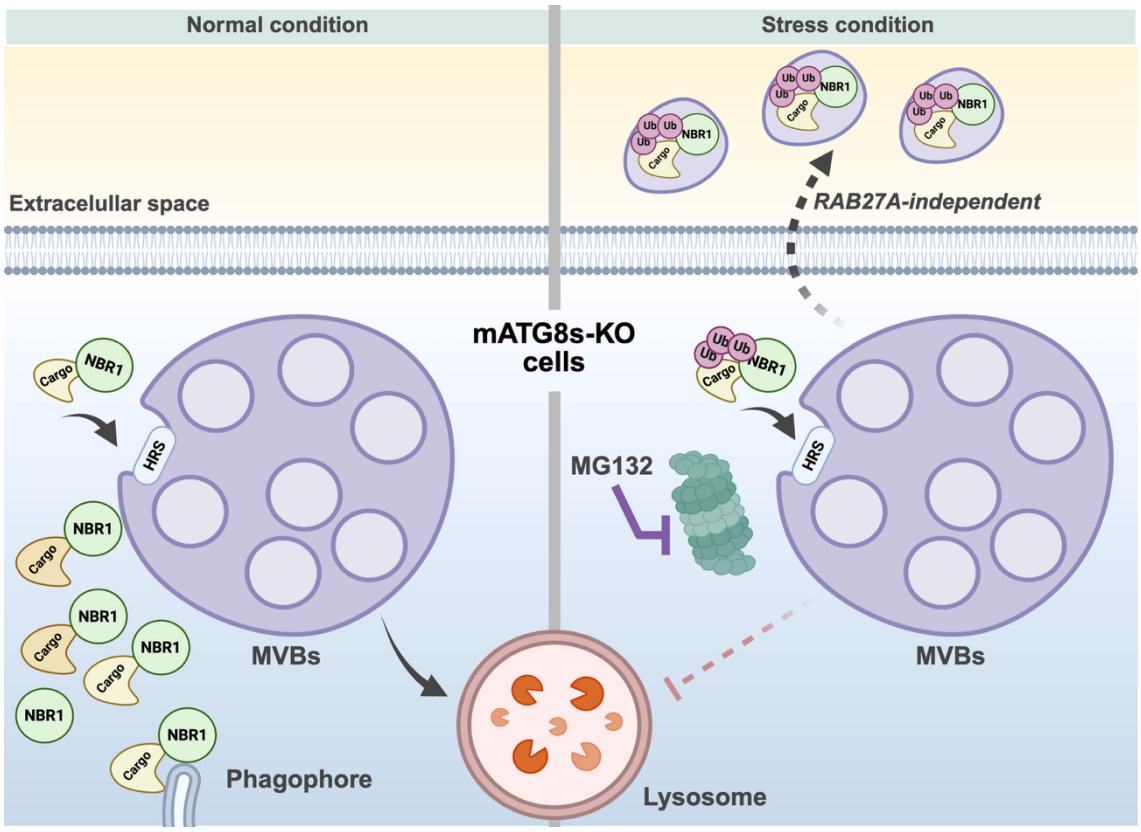

In the absence of mATG8s, NBR1 may be recruited to multivesicular bodies (MVBs) via HRS, for later degradation in lysosomes (left panel). Under proteasomal inhibition, NBR1 associated with MVBs (with ubiquitinated cargos) is downregulated, independent of lysosomes. Possibly, this downregulation is due to a secretion process, through a RAB27A-independent mechanism.

Abstract

Autophagy is a lysosome-dependent degradation process that involves autophagosome formation, typically mediated by mammalian ATG8 proteins (mATG8s). Autophagosomes can still form in their absence, suggesting alternative mechanisms. NBR1, a selective autophagy receptor, has been shown to compensate for autophagy defects. Here, we examined NBR1 regulation under proteotoxic stress in mATG8s-deficient HeLa cells. NBR1 levels were elevated in mATG8s knockout (KO) cells under basal conditions but decreased significantly after treatment with the proteasome inhibitor MG132. This reduction was not prevented by lysosomal inhibition with BafA1, indicating a non-lysosomal mechanism. Silencing of RAB27A reduced basal NBR1 levels, and the effects of MG132 were no longer observed, likely due to already diminished NBR1. Remaining NBR1 localized to puncta positive for ubiquitin and the ESCRT-0 component HRS, suggesting involvement of a ubiquitin-dependent endosomal pathway. Overall, our results suggest that under proteotoxic stress and impaired autophagy, cells activate alternative routes, potentially involving unconventional secretion, to regulate NBR1 levels.

Introduction

(Macro)Autophagy is a catabolic process that delivers cytoplasmic components to the lysosome for degradation through double-membrane autophagosomes. Its biogenesis requires the coordinated action of autophagy-related (ATG) proteins. In yeast, ATG8 is essential for autophagosome formation (1), while in mammals, this function is fulfilled by ATG8 orthologs (mATG8s), including LC3 and GABARAP protein families. Notably, unlike yeast, mammals can form autophagosomes even in the absence of mATG8s (2). Selective cargo recognition is mediated by autophagy receptors such as NBR1 and SQSTM1/p62 (3). In the absence of mATG8s, cargo can instead be secreted via autophagy-dependent secretion (4). Notably, NBR1 compensates for the loss of ATG7, an essential protein involved in mATG8s lipidation by promoting autophagosome formation through an alternative mechanism (5).

Given the central role of NBR1 in coordinating selective autophagy and potential compensatory pathways, we explored how NBR1 behaves under conditions of proteasomal inhibition in the absence of mATG8s. For this, HeLa cells, both WT and mATG8s KO, were compared, revealing that mATG8s KO cells displayed elevated levels of NBR1 relative to WT. Surprisingly, proteasomal inhibition with MG132 led to a significant decrease in NBR1 levels in mATG8s KO cells. Inhibiting lysosomal degradation using BafA1 failed to prevent this reduction, suggesting a non-lysosomal mechanism. Moreover, silencing of RAB27A, a GTPase involved in endo-lysosomal vesicle trafficking and secretion, reduced basal NBR1 levels and abolished its further decrease by MG132, likely due to already diminished levels rather than a requirement for RAB27A. Residual NBR1 localized in punctate structures positive for ubiquitin and the ESCRT-0 component HRS, suggesting a ubiquitin-dependent endosomal mechanism. Altogether, these findings suggest that under proteotoxic stress and impaired autophagy, cells engage alternative pathways, potentially involving unconventional secretion of NBR1.

Methods

Reagents and Antibodies

MG132 (cat#47479), Bafilomycin A1 (BafA1, cat#B1793), anti-NBR1 (cat#sc-130380, NBP171703), anti-EEA1 (cat#61045), anti-CD63 (cat#ab8219), anti-Cathepsin D (cat#AF1014), anti-HRS (cat#ab15539), anti-ubiquitin (cat#AUB01), and anti-RAB27A (cat#168013) were used.

Cell Culture, Treatments, and Western Blot

HeLa WT and mATG8s KO cells (courtesy of Dr. Maho Hamasaki, Osaka University), and HEK293T cells (cat#632180), were cultured in DMEM High Glucose (cat#12800-017) supplemented with 10% heat-inactivated FBS (cat#sv30160.03), 100 U/mL penicillin, and 100 µg/mL streptomycin (cat#15070-063), at 37°C and 5% CO_2. Cells were seeded after trypsinization with 0.05% trypsin and 1 mM EDTA (cat#25300-54).

For treatments, cells were incubated with 10 µM MG132 for 8 h or 100 nM BafA1 for 4 h. DMSO was used as vehicle control.

Cells were washed with cold PBS (cat#46-013) and lysed in RIPA buffer [50 mM Tris-HCl, 150 mM NaCl, 5 mM EDTA, 1% NP-40, 1% sodium deoxycholate, 0.1% SDS, pH 7.4] supplemented with protease inhibitors (cat#P8340). Lysates were sonicated on ice (3

121 pulses, 2–3 s, 40 mA) and processed for SDS-PAGE, Western blotting, and membrane
122 detection following previously described protocols (6).
123
124 *Immunofluorescence and Confocal Microscopy*
125 Cells grown on coverslips were fixed, permeabilized, and stained as previously described
126 (6). Images were acquired using a Leica TCS SP8 confocal microscope (6).
127
128 *Lentiviral Transduction and Stable Knockdown*
129 RAB27A knockdown was achieved by lentiviral transduction with shRNA as previously
130 described (6). mATG8s KO cells were selected with 6 µg/mL puromycin (cat#P8833).
131 Knockdown efficiency was confirmed by Western blot.
132
133 *Data Analysis*
134 Densitometry and image quantification were performed using FIJI (ImageJ), Excel 2022,
135 and Prism 10.0 (macOS). Statistical significance was determined using a one-tailed t-
136 test.
137
138 **Results**
139
140 <u>Proteasomal inhibition with MG132 reduces NBR1 levels in HeLa cells lacking mATG8s</u>
141 <u>proteins, independently of lysosomal degradation</u>
142 The absence of mATG8s in HeLa cells perturbs autophagosome trafficking, alters their
143 morphology, and slows down their biogenesis rate (2), ultimately leading to the
144 accumulation of selective autophagy receptors. Consistent with this, we confirmed the
145 accumulation of NBR1 in mATG8s-KO HeLa cells compared to wild-type (WT) by Western
146 blot analysis (Fig. 1A, lanes 1 and 3; Fig. 1B). Considering that in mATG8s-KO cells, cells
147 may rely on the proteasomal system to maintain proteostasis, where NBR1 can promote
148 substrate delivery to the proteasome, we explore whether proteasome inhibition
149 increases NBR1 levels. Contrary to our expectations, treatment with 10 µM MG132 for
150 8 h led to a significant decrease in NBR1 protein levels in mATG8s-KO cells, as shown by
151 Western blot (Fig. 1A line 3 and line 4; Fig. 1B) and immunofluorescence (Fig. 1C and
152 1D), a phenotype that was not observed in WT cells. Proteasome inhibition is known to
153 activate lysosomal biogenesis and autophagosome degradation (7). We tested whether
154 the reduction in NBR1 levels was due to lysosomal degradation. Cells were treated with
155 10 µM MG132 for 8 h, with 100 nM BafA1 added during the final 2 h to inhibit lysosomal
156 activity. Lysosomal inhibition did not restore NBR1 levels in mATG8s-KO cells (Fig. 1E
157 and 1F), indicating that the MG132-induced decrease in NBR1 is not mediated by
158 lysosomal degradation.
159
160 <u>Residual NBR1 levels in response to catalytic proteasome inhibition co-localize with</u>
161 <u>ESCRT-0 component HRS and Ubiquitin aggregates.</u>
162 To gain insight into the trafficking pathways involved, we next assessed the subcellular
163 distribution of NBR1 following MG132 treatment. Given that NBR1 can be incorporated
164 into endosomes under basal conditions in yeast (8), we evaluated its co-localization with
165 markers of the endolysosomal pathway in mATG8s-KO cells treated with MG132,
166 including early endosomes (EEA1), the ESCRT-0 component HRS (involved in endosomal
167 sorting (9)), late endosomes (CD63), and lysosomes (Cathepsin D, CathD). Confocal
168 microscopy analysis revealed a significant co-localization of NRB1 with HRS, compared

169 to the other markers (Fig. 2A and 2B), predominantly within large circular structures (Fig.
170 2A, arrowheads). Since NBR1 recognizes ubiquitinated cargos for degradation, we next
171 examined the co-localization of NBR1 and HRS with ubiquitin following proteasome
172 inhibition in mATG8s-KO cells. Confocal analysis showed that both NBR1 and HRS co-
173 localize with ubiquitin after MG132 treatment (Fig. 2C and 2D), within similar structures.
174
175 Proteasomal inhibition with MG132 reduces NBR1 levels in mATG8-KO cells, via a
176 RAB27A-independent mechanism.
177 Given the observed association between HRS and NBR1 after proteasome inhibition,
178 and that HRS mediates earlier steps in intraluminal vesicle formation at endosomes,
179 later released as exosomes via MVB-plasma membrane fusion regulated by the GTPase
180 RAB27A (9), we investigated whether NBR1 reduction could be mediated by RAB27A-
181 dependent secretion. To test this, we generated stable RAB27A knockdown in mATG8s-
182 KO cells via lentiviral transduction (shRAB27A), using cells expressing a shRNA against
183 luciferase as a control (shLuc). Western blot analysis revealed reduced basal NBR1 levels
184 in shRAB27A compared to shLuc cells (Fig. 2E, lanes 1 and 3; Fig. 2F). We next assessed
185 the effect of proteasome inhibition in these lines. As expected, MG132 treatment
186 reduced NBR1 levels in shLuc cells (Fig. 2E, lanes 1 and 2; Fig. 2F). In contrast, MG132
187 treatment did not further decrease NBR1 levels in shRab27A cells (Fig. 2E, lanes 3 and
188 4; Fig. 2F), suggesting that the reduction of NBR1 upon proteasomal inhibition occurs
189 through a RAB27A-independent mechanism.
190
191 **Discussion**
192 Here, we show that NBR1 protein levels, elevated in mATG8s-KO cells, decrease under
193 two distinct stress conditions: proteasomal inhibition and RAB27A silencing. The
194 remaining NBR1 signal localizes to dot-like structures that co-localize with the ESCRT-0
195 component HRS and ubiquitin, suggesting involvement of the ubiquitin-dependent
196 endosomal pathway. Consistent with this, lysosomal inhibition using BafA1 did not
197 restore NBR1 levels, and no intracellular accumulation was observed, supporting the
198 notion that its reduction is not due to lysosomal degradation. RAB27A silencing in
199 mATG8s-KO cells also reduced NBR1 levels, suggesting that in the absence of this
200 GTPase, NBR1 may be rerouted toward degradation or secretion via yet unidentified
201 mechanisms. Although we did not directly assess secretion, our findings align with the
202 possibility that NBR1 is released via a non-canonical pathway under cellular stress. The
203 absence of MG132-induced NBR1 reduction in RAB27A-silenced cells likely reflects
204 already diminished basal levels due to RAB27A depletion, rather than indicating its
205 requirement in the MG132 response. Thus, NBR1 downregulation upon proteasome
206 inhibition likely proceeds through a RAB27A-independent mechanism.
207
208 These results suggest that when canonical autophagy is compromised, cells become
209 more vulnerable to additional stressors such as proteasome inhibition or vesicular
210 trafficking disruption. In compensation, they may activate alternative pathways
211 involving selective autophagy receptors that bind ubiquitinated cargo, with HRS
212 potentially contributing. HRS has been implicated in autophagy-dependent secretory
213 autophagy, typically requiring LC3 (10). However, our data point to an LC3-independent
214 mechanism, consistent with the absence of mATG8s, where NBR1 may be redirected

into ubiquitin-enriched vesicles. Whether these vesicles are ultimately secreted, and the nature of the underlying pathway, remain to be determined.

Given that aging and chronic proteotoxic stress impair canonical autophagy, identifying alternative routes for protein handling may offer new insights into cellular resilience and protein quality control.

262 **Figures and leyends**

263

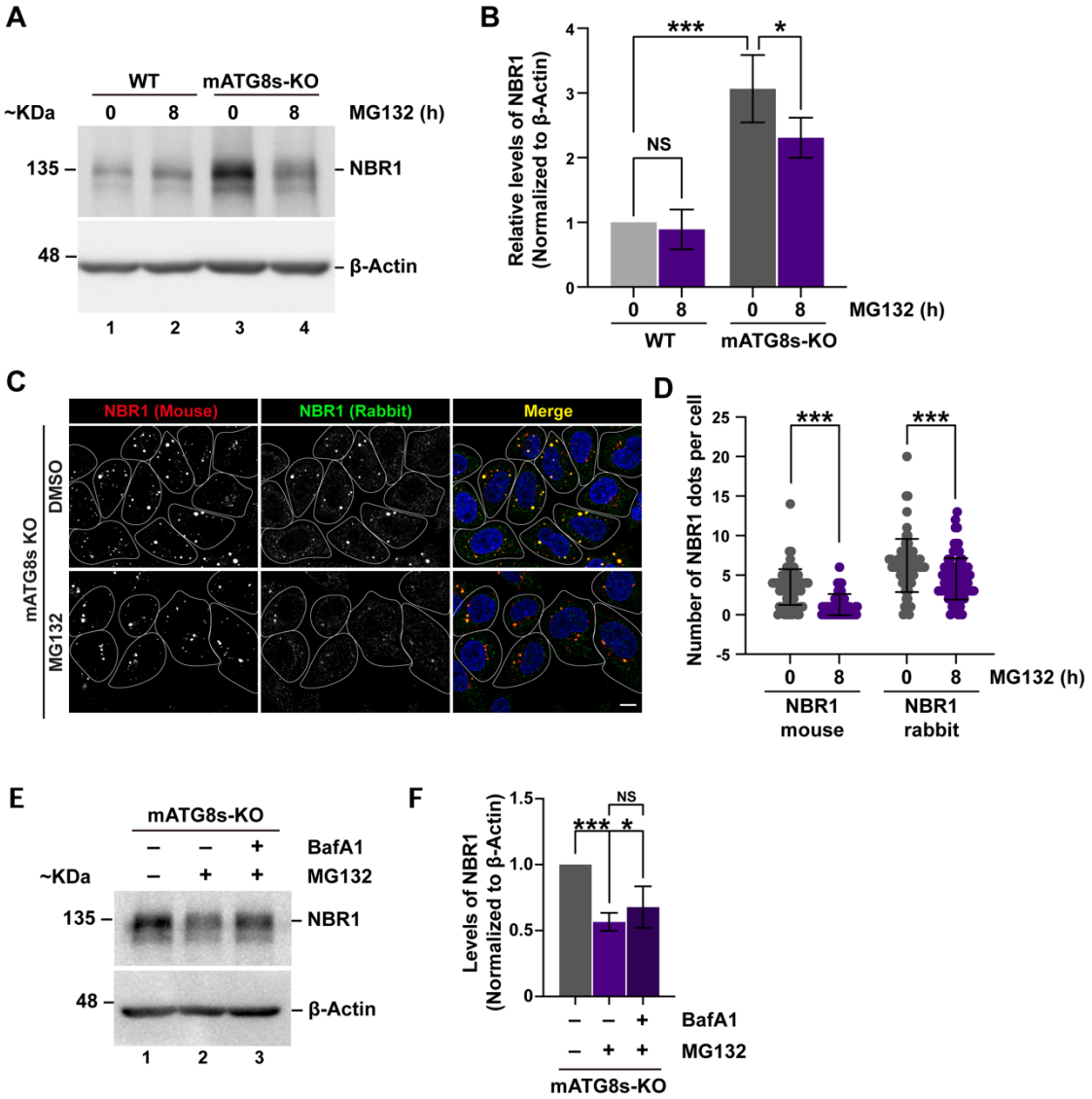

Figure 1
Cerda-Troncoso C, et al., 2025

264

265 **Figure 1**. Catalytic proteasome inhibition reduces NBR1 levels in mATG8-deficient cells.
266 (A) Western blot of endogenous NBR1 and β-actin in HeLa WT and HeLa mATG8s KO
267 cells treated with 10 µM MG132 for 0 or 8 h. Cells were lysed with RIPA buffer. (B)
268 Densitometric quantification of NRB1 levels shown in (A). NS: No-Significative **P<0.01,
269 ***P<0,001; unpaired-parametric t-Test. (C) Immunofluorescence analysis of NBR1
270 distribution in HeLa WT and HeLa mATG8s-KO cells treated with 10 µM MG132 for 0 or
271 8 h; Scale bar 10 µm. (D) Quantification of NBR1 positive puncta per cell from images in
272 (C); ***P<0,001; unpaired-parametric t-Test. (E) Western blot of endogenous NBR1 and

β-actin in HeLa mATG8s KO cells treated with 10 µM MG132 for 0 or 8 h, with or without 100 nM BafA1 added during the final 2 h. (F) Densitometric quantification of NBR1 levels from (E); NS: No-Significative, *P<0.05, ***P<0.001; unpaired-parametric t-Test.

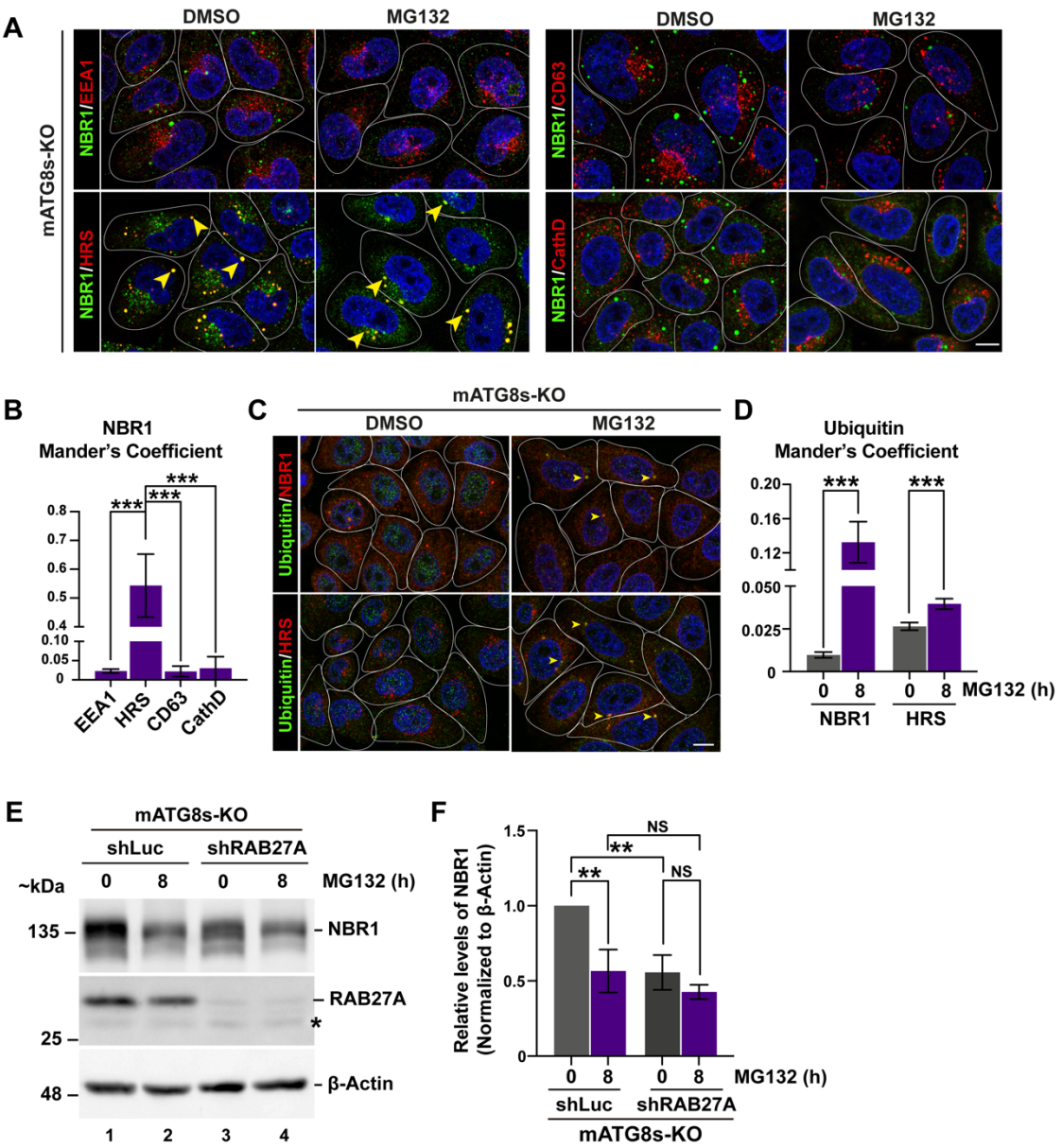

Figure 2
Cerda-Troncoso C, et al., 2025

Figure 2. Residual NBR1 localizes to HRS and ubiquitin structures following catalytic proteasome inhibition. (A) Confocal analysis of NBR1 with endolysosomal markers in mATG8s KO cells treated with 10 µM MG132 for 0 or 8 h. Markers include EEA1 (early endosomes), HRS (MVBs), CD63 (secretory MVBs), and CathD (lysosomes); arrowheads indicate areas of co-localization. (B) Representative quantification of NBR1 co-localization with HRS from panel (A). (C) Mander's coefficient quantification of NBR1 co-localization with the indicated endolysosomal markers after MG132 treatment; ***P<0.001; unpaired-parametric t-Test. (D) Confocal analysis of NBR1 or HRS co-localization with ubiquitin after 0 or 8 h of 10 µM MG132 treatment in mATG8s KO cells;

arrowheads show co-localization. (D) Mander's coefficient quantification of ubiquitin co-localization with NBR1 or HRS following MG132 treatment as shown in (C); ***P<0.001; unpaired-parametric t-Test. (F) Western blot analysis of NBR1 and β-actin protein levels in mATG8s KO either shLuc and shRAB27A cells, treated with 10 µM MG132 for 0 or 8 h. (G) Densitometric quantification of Western blot shown in (F); NS: No-Significative **P<0.01; unpaired-parametric t-Test.

References

1. Nakatogawa H, Ichimura Y, Ohsumi Y. Atg8 controls phagophore expansion during autophagosome formation. Mol Biol Cell. 2008 Jul;19(7):3290-8. doi: 10.1091/mbc.E07-12-1292. PMID: 18508918.
2. Nguyen TN, Padman BS, Usher J, Oorschot V, Ramm G, Lazarou M. Atg8 family LC3/GABARAP proteins are crucial for autophagosome-lysosome fusion but not autophagosome formation during PINK1/Parkin mitophagy and starvation. J Cell Biol. 2016 Dec 19;215(6):857-874. doi: 10.1083/jcb.201607039. PMID: 27864321.
3. Vargas JNS, Hamasaki M, Kawabata T, Youle RJ, Yoshimori T. The mechanisms and roles of selective autophagy in mammals. Nat Rev Mol Cell Biol. 2023 Mar;24(3):167–85. doi:10.1038/s41580-022-00542-
4. Tan HWS, Luo S, Wang Z, et al. A degradative to secretory autophagy switch mediates mitochondria clearance in the absence of the mATG8-conjugation machinery. Nat Commun. 2022 Jun 28;13:3720. doi: 10.1038/s41467-022-31213-7. PMID: 35764633.
5. Shoemaker CJ, Huang H, Weir NR, et al. Receptor-mediated clustering of FIP200 bypasses the role of LC3 lipidation in autophagy. EMBO J. 2020 Nov 23;39(23):e104948. doi: 10.15252/embj.2020104948. PMID: 33226137.
6. Cerda-Troncoso C, et al. Chemo-small extracellular vesicles released in cisplatin-resistance ovarian cancer cells are regulated by the lysosomal function. J Extracell Vesicles. 2024 May 30;13(5):e12338. PMID: 38947172. Sep;24(18):8055-68. doi: 10.1128/MCB.24.18.8055-8068.2004. PMID: 15340068.
7. Zhang X, Garstka MA, Wang Z, et al. Proteasome Inhibition Activates Autophagy-Lysosome Pathway and the Formation of Aggresome in Human Mature Dendritic Cells. Front Cell Dev Biol. 2019;7:282. doi: 10.3389/fcell.2019.00282. PMID: 31508418.
8. Liu XM, Sun LL, Hu W, Ding YH, Dong MQ, Du LL. ESCRTs cooperate with a selective autophagy receptor to mediate vacuolar targeting of soluble cargos. Mol Cell. 2015 Sep 17;59(6):1035–42. doi:10.1016/j.molcel.2015.07.034. PMID:26365378.
9. Hessvik NP, Llorente A. Current knowledge on exosome biogenesis and release. Cell Mol Life Sci. 2018 Jan;75(2):193-208. doi: 10.1007/s00018-017-2595-9. PMID: 28733901.
10. Leidal AM, Huang HH, Marsh T, Solvik T, Zhang D, Ye J, Kai F, Goldsmith J, Liu JY, Huang YH, Monkkonen T, Vlahakis A, Huang EJ, Goodarzi H, Yu L, Wiita AP, Debnath J. LC3-dependent EV loading and secretion (LDELS) promotes TFRC secretion and microenvironment remodeling. Nat Cell Biol. 2023 May;25(5):741-754. doi: 10.1038/s41556-023-01154-3. PMID: 36286616.